Polymer Bulletin (2026) 83:69
https://doi.org/10.1007/s00289-025-06081-y

ORIGINAL PAPER

# Numerical scaling approaches for the irreversible formation of carbon nanotube reinforced polyester-based nanocomposites

**Mehmet Bayırlı**[1] · **Aykut Ilgaz**[1]

Received: 7 April 2025 / Revised: 20 September 2025 / Accepted: 12 November 2025 /
Published online: 10 December 2025


## Abstract

The internal structure and characteristic properties of pure and carbon nanotube filled composites are closely dependent on the properties of the substances added for production, their weight% in the material, and the production process. The different properties of the components in the material and the variability of production parameters cause the observable surface structures of the produced samples to exhibit self-similar characteristics. This repetition behavior shapes the permeability properties of materials as well as morphological changes. In order to understand the multiple surface structuring of the materials and the characteristic changes it brings, the surfaces of the samples produced with the sheet molding compound (SMC) technique were examined using a scanning electron microscope (SEM). SEM analysis results revealed that the correlation length of the cluster size within the surface structure showed unique fractal scaling behaviors. Universal critical exponent values and fractal dimensions were calculated using the scaling method and numerical approaches to determine the change of the root mean square roughness (rms), which was used as a statistical measure of the surface change of the samples. It was found that the probability distribution in the model proposed for multicluster formation conforms on an exponential distribution and the structuring process of the samples is determined by the Poisson process. It is predicted that the structuring process involves an irreversible, physical and chemical mechanism.

**Keywords** Fractal analysis · Single-walled carbon nanotube · Morphological variations · Poisson process

✉ Aykut Ilgaz
aykut17ilgaz@gmail.com

[1] Department of Physics, Faculty of Science and Letter, Balıkesir University, Çagıs Kampüsü, Balıkesir 10185, Turkey

## Introduction

In recent years, many studies have been conducted on the addition of carbon nanotubes to composites due to their unique properties and the advantages they bring. The focus of the studies is on the effect of the production method, the resin used and the doping ratio on the mechanical, electrical and thermal properties of nanotube doped composites. However, there have not been enough studies yet on the heterogeneous morphological multiple internal structure and fractal characteristics of polymer materials. The morphological internal structure of the composite depends on the production method, material type and quantities. In such materials, it is observed that the structure generally has multiple morphologies in superficial two-dimensional (2D) and volumetric three-dimensional (3D) observations [1, 2]. The dense structure, which varies regionally in interdependent or independent clusters, includes long finger arrays of fibers, mountain and valley-like and partially dendritic-shaped formations.

Fractal analysis concepts with scaling method are used in the literature to determine the morphological formations and statistical behavior of composites [3–6]. The macrostructuring of multiple morphological surfaces is characterized by a fractal dimension term that is different from the Euclidean dimension and is not an integer. To determine the fractal dimension, algorithms have been developed that give different characteristic results such as box size, similarity dimension, Hausdorff dimension and spectral density. In addition to the internal structure, the structures on the composite surfaces are also determined using statistical scaling approaches. By using these methods, which will provide different perspectives, universal critical exponent values that characterize structuring can be calculated. Root mean square roughness (rms), fractal dimension, cluster-size distribution function and power-law relationship of the number of clusters, which represent pixel-sized particle clusters in micro images, are also characteristic parameters that can be obtained with these methods [5–9]. Ilgaz and Bayırlı suggested that the cluster patterns of pure and CNT-reinforced composites can be examined with fractal approaches, based on the superficial cluster formations. They also revealed that there are repetitions of self-similar structures in the micro images of composite surface aggregates [10]. Such studies are critical not only for a better understanding of the structuring mechanisms of composites, but also for the preparation of some thin films containing special physical and chemical properties.

Agglomeration is especially important for composites, CNT-doped composites and thin film structures produced by electrodeposition. It is possible to determine the structure of their heteromorphology from the surfaces observable by scanning electron microscope (SEM). In addition, both experimental and simulation studies are carried out to identify independent clusters in surface structures. Two of the most notable of these are interrelated diffusion-limited aggregation (DLA) [11, 12] and diffusion-controlled deposition (DCA) models [9]. These proposed models have broken new ground in describing the structures formed by particles clustering, especially in the dendritic structure. Then, the simulation of the macro structure of densely structured clusters was developed by adding the activation energy for reactions in the structuring process of the materials and the adhesion probability parameter, which

was introduced to determine the clustering formed by particles by reducing irreversible ions, to these models [11]. Although these models cannot explain crystalline structuring in morphological structuring, statistical parameters can be determined with the scaling method of the cluster representations produced.

The aim of this study is to reveal the heterogeneous morphological aggregation structure on the surfaces of pure and SWCNT-doped composite materials. For this purpose, the root-mean-square roughness (rms) values of the particle clusters in the structure were calculated for both undoped and doped samples, and their universal critical exponent values were determined. In addition, fractal dimensions, which are critical parameters, were calculated and a numerical model was proposed by defining the probability density function and cluster-size distribution function for the clusters. The results obtained are compared with thin film samples and different types of composite surface aggregation samples, according to the scaling theory.

## Material and method

### Material

SWCNT with an average length of 19 μm was provided by OCSiAl-Tuball Matrix/Germany. 1 wt% SWCNTs were sonicated for 1 h at room temperature to obtain a comprehensive dispersion before adding them to the sample (Branson Ultrasonic Bath). Then, carbon nanotubes were added to the orthophthalic-based polyester resin and the resulting suspension was placed in the ultrasonic bath again. Applying sheet molding compound (SMC) technique, zinc sulfide, thickening mixture, styrene, calcium carbonate (wt% 30) and glass fibers (wt% 27), which will give strength to the material, were added to the mixture. In addition, tetrahydrophthalic anhydride and benzyldimethylamine components were used as hardeners and catalytic materials in the mixture. Finally, the mixture containing all these components was poured into molds of appropriate size and kept at room temperature.

### Method

SEM images obtained from the PC and SWCNT added composite were transferred to the computer environment with the ImageJ 1.53t program and analyzed by applying the Gaussian filter ($\sigma = 2$) in the pre-processing [13]. Images were digitized using the 'IsoData' thresholding algorithm, converted to 8-bit grayscale. 'Watershed' segmentation was used to separate adjacent clusters [14]. Binary images were used as data in calculating the pixel density of the clusters. The process steps were as follows:

(i) Gaussian Blur: A Gaussian filter was applied with $\sigma = 2$.
(ii) Thresholding Algorithm: Digitized using "IsoData" (iterative histogram analysis).
(iii) Binary Image Creation: 8-bit gray level → automatic thresholding was applied in the 45–99% brightness range.
(iv) Segmentation: Adjacent clusters were separated using the "Watershed" algorithm.

(v) Validation: Visual inspection + Regression coefficients ($r^2 > 0.97$) were calculated.

In summary, to increase the statistical reliability and transparency of the regression analyses presented in this study, 95% confidence intervals were added to all log-log plots and cluster size distribution plots. Each fitted curve is accompanied by an $R^2$ (coefficient of determination) value indicating the degree of compatibility. Error bands were added where appropriate to indicate the uncertainty around the regression line. Monte Carlo resampling with 10,000 iterations and nonparametric bootstrap methods were applied to estimate statistical variability and verify the robustness of the observed scaling behavior. These approaches allow estimation of critical exponent values and confidence intervals for regression parameters, particularly for sparse data points and high-density regions.

## Results and discussion

In statistical physics, the concepts of scaling and self-similarity are important to determine the structuring and phase transitions in any morphological formation such as composites and thin films. In particular, the scaling method can be determined by laws containing simple exponent values, independently of the characteristics of the experimental systems and the values of the production conditions. The structuring of composites produced with SMC; it creates morphological phase transitions from sparse structure to dense structure, depending on the production method and production process and the components it contains. Therefore, the scaling method can be used to investigate the superficial observable microstructuring of the composites produced for this study.

In order to observe the superficial structuring of the pure material in RGB format, the materials were first scanned with SEM and 3D topographic images were obtained as seen in Fig. 1(a) and 1(b). The rectangular mesh dimensions of this sample are 533.68 μm x 361.05 μm (1024 pixels x 686 pixels, 8 bit, magnification 5.00 Kx) at an image resolution of 1.9 μm/pixel. Figure 1(c) also shows typical power spectrum image in frequency space found by the Fast Fourier Transform (FTT) for neat material. In the last part the images were edited in 8-bit gray scale and converted to bitmap format shown in Fig. 1(d) to apply statistical calculations of cellular particle density and cluster structuring. Similar graphs were prepared for the nanotube filled sample and are presented in Fig. 2(a), 2(b), 2(c) and 2(d). When the surfaces of the samples were examined, it was observed that they had an amorphous structure, but there was no symmetrical structure in general. In the surface structure, the structure is formed by glass fibers lying partially cylindrically parallel to each other and other components, especially $CaCO_3$, settled between them; it is observed that island, mountain and valley-like appearances are formed. The difference in cellular and regional brightness of the image patterns is thought to be due to the heterogeneous distribution of resin and components in the matrix.

When the micro images of the superficial poly morphological structures of pure and doped structures are examined, clusters that are dependent and independent from each other are observed. If the digitized micro BMP image surface particle clusters

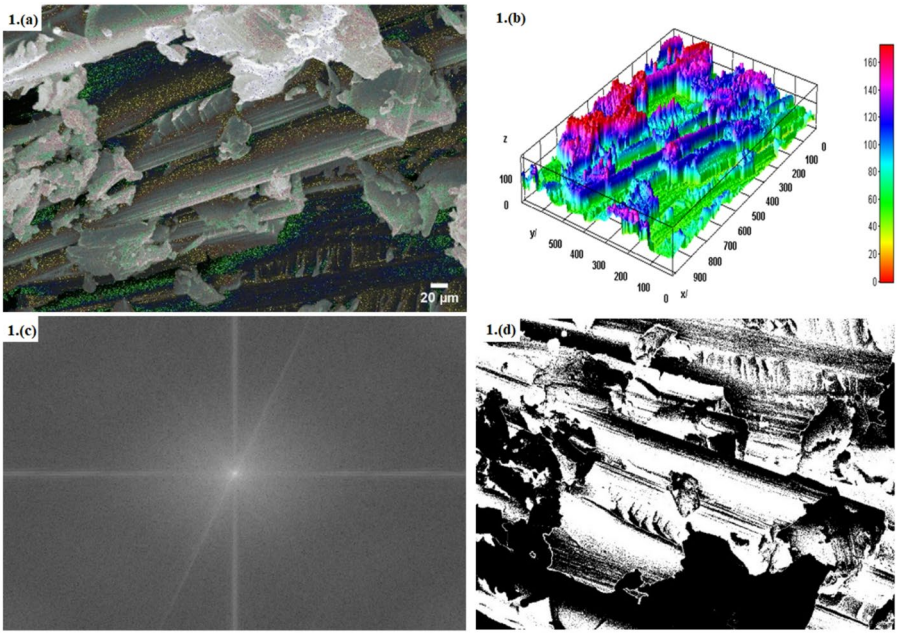


**Fig. 1** (**a**) Micro SEM image of pure polyester composite, (**b**) topographic 3D structuring, (**c**) Typical power spectrum image in frequency space obtained from the original image. This image was obtained using the Fast Fourier Transform (FFT) technique shown in (**a**), (**d**) BMP format image

are optimized to an approximate ellipse format, it is possible to partially observe the components and SWCNT aggregations. Figures 3(a) and 3(b) show the poly structuring of pure and doped samples, respectively. Elliptical structures corresponding to possible clusters of the production materials are clearly observed. From this observation, it can be said that nanotubes are structured as ribbons on the surfaces of the fibers and in the resin.

In addition to digitized image processing, two different methods were used for the fractal characterization of surface morphology in this study. The first involves calculating critical exponential values (α and β) using log-log regression based on the scaling law. The critical exponents describe universal aspects of morphological evolution in disordered systems such as composite materials. α reflects the evolution of surface roughness by characterizing the spatial correlation of cluster sizes. Higher α values characterize greater heterogeneity in the distribution of clusters in the structure [9, 15, 16]. The critical exponent β quantifies density fluctuations and interface scaling. The critical exponent β, which relates the root mean square roughness to the number of clusters, is sensitive to aggregation mechanisms (e.g., diffusion-limited and reaction-controlled) [8]. In this scaling approach, fractal dimensions are derived using the log-log relationship between cluster size and RMS data. The second is the box-counting method applied to SEM images. Statistical reliability was achieved for both methods, with regression coefficients $r^2 > 0.97$. The obtained fractal dimension values are consistent with those reported in the literature for similar structures [9, 17].

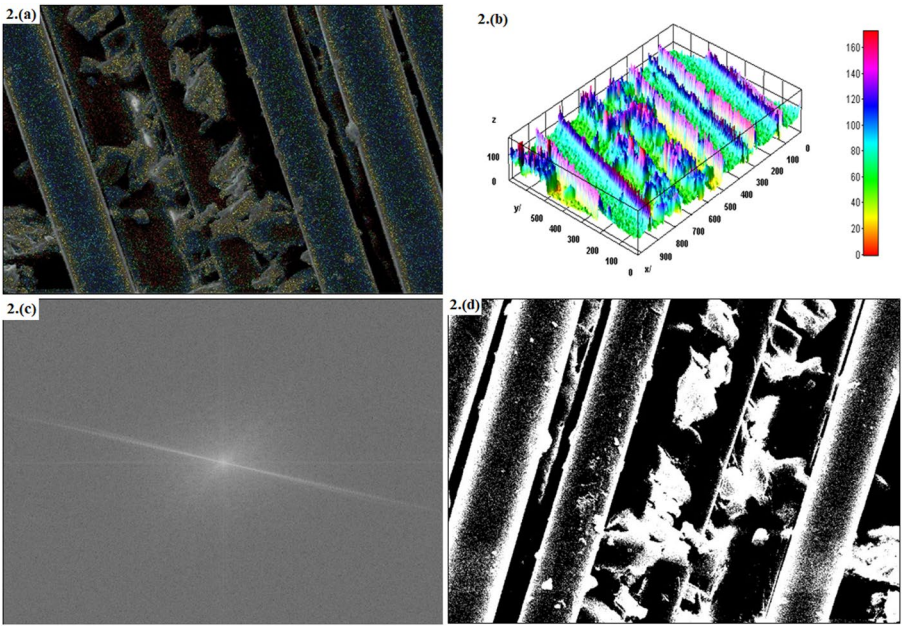


**Fig. 2** (**a**) Micro SEM image of SWCNT modified polyester composite, (**b**) topographic 3D structuring, (**c**) A typical power spectrum image in frequency space obtained from the original image. This image was obtained using the Fast Fourier Transform (FFT) technique shown in (**a**), (**d**) BMP format image

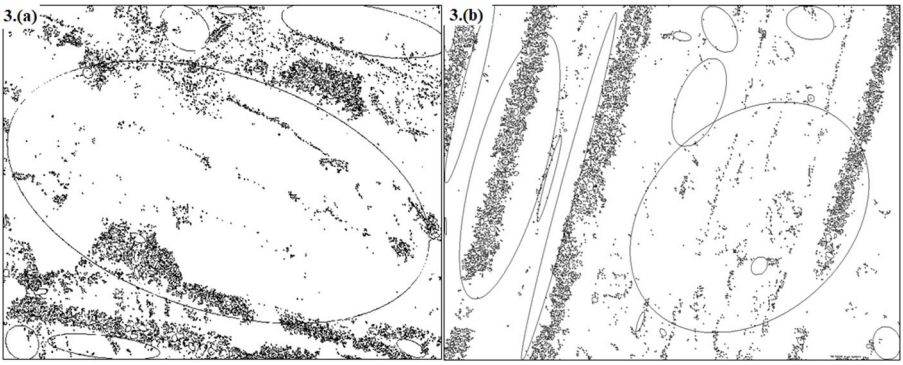


**Fig. 3** Multiple morphological structures of (**a**) Neat and (**b**) Nanotube doped polymer composites

The comparative presentation of these two different methods together is to increase the numerical integrity, reproducibility and reliability of the study.

While the statistical scaling parameters of the heterogeneous structures of composite materials are examined by the stochastic process method, interface critical exponent values and cluster size distribution functions must be calculated to determine the poly morphological structures [8, 9]. The root mean square roughness (rms) value of the $s_i$ sizes of the clusters formed independently of each other by the pixels

representing the matrix containing resin and SWCNT of size $\epsilon_i \in R^+$ can be defined by the following relation:

$$\mathrm{T}\,(\mathrm{h}) = \langle \mathrm{s_i} - \langle \mathrm{s_i} \rangle \rangle^{1/2} \tag{1}$$

This rms value shows an average value over the number of pixels under the region that determines the T(h) roughness, and the sum of the cluster sizes formed by the cumulative pixels is the sum of the particle densities. The cluster size and the number of clusters in the range in which the clusters exhibit scaling behavior are determined as follows:

$$\mathrm{s_i} = \sum_{\mathrm{x_i} \leq \mathrm{s_i}} \mathrm{k_j}.\rho\,(\epsilon_\mathrm{i}) \text{ and } \mathrm{N}\,(\mathrm{s_i}) = \sum_{\mathrm{s_i} \leq \mathrm{h}} \mathrm{f}.\mathrm{k_j}.\rho\,(\epsilon_\mathrm{i}) \tag{2}$$

where $\mathrm{k_j}$ is the sum of the particle densities in each cluster and f is the number of repetitions of the cluster of size $\mathrm{s_i}$ on the surface. While the cluster size is calculated in the range of 1 to 254,987 for the pure sample, it takes values ranging from 1 to 242,536 for the nanotube reinforced sample. 5326 independent clusters were determined for the pure sample, and this number was estimated as 16,133 for the doped sample. This result shows that the cluster formation of composite materials increases irregularly when SWCNT is added. The particle density is also denotes as follows;

$$\rho\,(\epsilon_\mathrm{i}) = \begin{cases} \text{if a dark piksel exists at } \epsilon_\mathrm{i}\ 1, \\ \text{else a brigth piksel exists at } \epsilon_\mathrm{i}\ 0. \end{cases} \tag{3}$$

where $\epsilon_\mathrm{i}$ is the pixel size representing unit particle density. The probability of the components other than the cylindrical glass fibers seen in Figs. 1(a) and 1(b) being present on the rectangular mesh surface (covering rate) can be determined by the following equation:

$$\mathrm{P_{pure}}\,(\epsilon_\mathrm{i}, (\mathrm{LxM})) = (\mathrm{LxM})^{-1} \sum\nolimits_{\epsilon \leq \mathrm{s_i}} \rho\,(\epsilon_\mathrm{i}) \tag{4}$$

$$\mathrm{P_{SWCNT}}\,(\epsilon_\mathrm{i}, (\mathrm{LxM})) = (\mathrm{LxM})^{-1} \sum_{\epsilon \leq\ \mathrm{s_i}} \rho\,(\epsilon_\mathrm{i}) \tag{5}$$

where LxM is the edge dimension value of the rectangular mesh surface structuring. Coverage rate shows the effect of the components that can be observed effectively in the surface structure on the structure. Nanotube doping changes the structure and therefore the covering rate of the material. The covering rates were determined as 45.91% for pure material and 47.99% for SWCNT reinforced composite. The relationship between the rms value N(h) and h of the clusters formed by the observable pixels for both samples is as follows:

$$\mathrm{N}\,(\mathrm{h}) \sim\ \mathrm{h}^{\alpha} \tag{6}$$

where α is the primary critical exponent value that defines the cluster structures. Cluster structuring on the sample surfaces shows a scaling behavior with sizes ranging from $s_i < \sim 3$ pixels to $s_i < \sim 100$ pixels. The formation frequency of values after 100 pixels is quite low and the scaling behavior disappears. The primary critical exponent α was calculated by linear regression method by taking the logarithms of both axes. It was determined as α = 1.705 for the undoped sample and α = 1.965 for the CNT-doped sample. The relationship between the rms value T(h) and the cumulative number of clusters can be defined as follows:

$$T(h) \sim N(h)^{-\beta} \tag{7}$$

where β is the secondary critical exponent value that determines the structuring in the samples. Figure 4 shows the variation graph of T(h) with N(h) values, and the secondary critical exponent β value is calculated by linear regression method by taking the logarithms of both axes. While the calculations showed the β value for the pure sample as 0.481, the contribution of the carbon nanotube increased the β value in the sample to 0.519. In the studies conducted by Saitou et al., the primary critical exponent calculated for nickel phosphorus (Ni-P) thin film surfaces produced by the electrodeposition method under galvano-static conditions was calculated as α = 1.15 and the secondary critical exponent was calculated as β = 0.910 [15], and it was found to be in agreement with the values found in this study. Similarly, Mathushita et al. determined the second critical exponent value as β = 1.5, as an approximation to the fractal dimension, for zinc (Zn) dendrite formations structured on a one-dimensional electrode by the electrodeposition method [16]. Meakin also determined that the second critical exponent value varies between 1.275 and 1.303 depending on the number of clusters in the diffusion-controlled deposition model simulations which use the probability of adhesion to define fiber surface cluster formations and represent the behavior of irreversibly reduced ions [9]. Although the Ni-P thin film, Zn dendrite, fiber surface formations and cluster structures of the materials in this study are quite different from each other, the critical exponent values confirm the calculations by taking values in similar ranges.

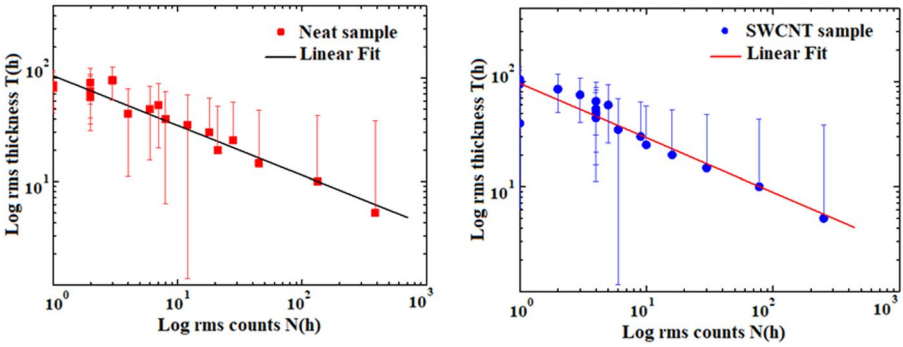


**Fig. 4** Variation of log N(h) value of (**a**) neat polyester composite (**b**) CNT-doped polyester sample depending on log rms roughness value

Depending on the cluster size and number of cumulative pixels on the material surfaces, the rms T(h) thickness is proportional to the independent cluster values. The $s_i$ values of the clusters are a random variable and have discrete values. $\overline{\epsilon_i} \sim h \sim \overline{s_i}$ expression implies that the projection of the poly morphology of the pixels can be determined approximately by h according to the image area. In this way, it is possible to determine a probability distribution function for clusters within the poly morphological structure. Although cluster sizes vary at variable values between $s_{min} = 1$ pixel and $s \to \infty$, each of them can take on finite and discrete values. The probability of observing each cluster of size $s_i$ is expressed as follows:

$$p(s_i) = P(S = s_i) \tag{8}$$

This value is proportional to the number of clusters $N(s_i)$ in the projection area of the rectangular mesh and cluster sizes with dimensions LxM. In addition, the probability mass function can be determined from the histogram graph, which determines the change of the number of clusters according to the value of $s_i$ according to the value of $N(s_i)$. Statistically, the sum of these probabilities is:

$$\sum_{i=1}^{N} P\ (s_i) = 1 \tag{9}$$

The probability of finding $s_i$ clusters on undoped and SWCNT-doped sample surfaces is defined as follows:

$$P_j\,(s_i) = (LxM)^{-1} N\,(s_i) \tag{10}$$

In this study, $N(s_i)$ is the number of clusters formed independently of each other by the cumulative pixels on the sample surfaces. According to the results obtained from the calculations of the average and standard deviation values of the cumulative pixels, it was determined that the approximate cluster mass was $m \sim h$ and $m^2 \sim s^2$. The expected value for the h values of the cumulative pixels implies that the probability distribution function $P_{ij}$ is significant if it exhibits an exponent distribution. Also, the relationship between the average value and standard deviation of the cluster size formed on the sample surfaces and observable from micro images is denoted as follows:

$$\overline{m} = \sum_{i=1}^{N} s_i p_j \tag{11}$$

and

$$\sigma^2 = \sum (s_i - \bar{s})^2 P_i \tag{12}$$

From the histogram graph given in Fig. 5, it was stated that the expected value of the cluster size $s_i \rightarrow \infty$ would be significant only in the case of the exponential probability distribution of $P(s_i)$. According to this condition, the probability distribution function is given by the following relation:

$$P_j(s_i) = h^{-1} e^{-\lambda s} \tag{13}$$

where $\lambda = h^{-1}$ is a tuning parameter for each sample. The exponential probability distribution revealed that the cluster structuring for both the pure and the doped sample showed a Poisson distribution. Therefore, it is possible to say that the sample production time and the superficial irreversible poly morphological structuring follows a Poisson spatial process.

Another approach is the cluster-size distribution function defined for cluster statistics in scaling theory. The change of cluster size on the sample surfaces according to the number of repetitions is shown in Fig. 5. The number of clusters on the nanotube sample surface is greater than that of the pure sample as long as $s_i < 5$ pixels. In addition, the cluster-size distribution function can be defined with the cluster size $s_i$ and the histogram values $N(s_i)$ corresponding to each cluster size by the following relation:

$$N(s_i, \lambda) = N(s_1) + c.e^{-\lambda s} \tag{14}$$

where $c = (k!)^{-1} \lambda^k$ is a constant, $\lambda = s\text{-}1$ is the expected value of the clusters formed on each sample surface as a positive real number, and k is the number of occurrences of the clustering event during production, given by the probability function. The function of k is a parameter for the Poisson distribution and can be defined as the probability mass function or cluster distribution function. Using the non-linear regression method, the constant value of the cluster size distribution function was calculated as $c = 26913.004 \pm 972.670$, $\lambda = -3.103 \pm 0.069$ for pure and $c = 33319.075 \pm 1078.245$,

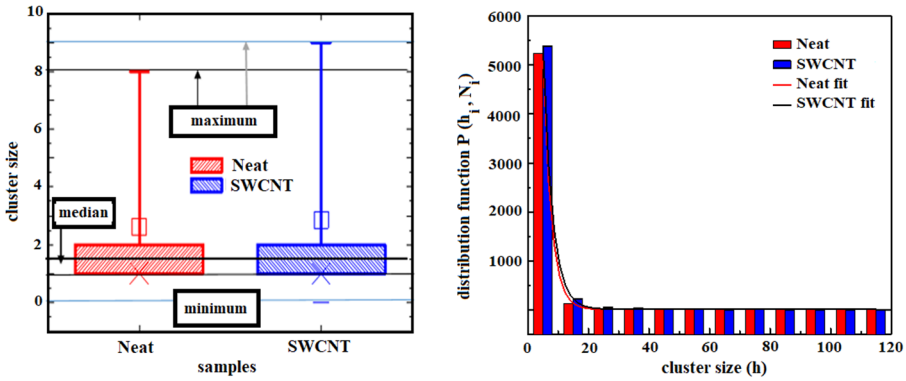


**Fig. 5** Histogram diagram of the variation in the number of clusters on sample surfaces with cluster size. Additionally, the cluster-size distribution function is shown using the non-linear regression method. When the histogram diagram is examined, the number of clusters with $s_i < \sim 5$ pixel value increases when CNT is doped

$\lambda = -2.701 \pm 0.047$ for SWCNT reinforced matrix. The validity and reliability of the model was checked with the regression coefficient, and the regression constants of the cluster-size distribution functions of the samples were determined as $r^2 > 0.99$ and the validity of the model was accepted. In addition to the regression constants, the values calculated in this study are summarized and given in Table 1.

In cluster statistics, there is a relative measurement uncertainty in the calculation of each value. Accordingly, the measurement uncertainty can be defined by the relation $\frac{\Delta d_f}{\overline{d_f}}$ and $\Delta d_f = d_f - \overline{d_f}$ is the standard deviation. Measurement uncertainties for each value of cluster statistics are also given in Table 1. The samples contain heteromorphologically structured layers containing partial gaps in d-dimensional space. In order to understand these structures and the sizes of the components, fractal dimension $d_f(d, d_b)$ values, one of the structuring parameters of the samples, are calculated using the scaling method. Fractal dimension ($d_f$) is a parameter that measures how cluster structures deviate from Euclidean geometry and occupy space, transforming morphological complexity into numerical data. Fractal dimension values between 1 and 2 (for 2D projections) express self-similarity in diffusion-limited aggregation (DLA) [11] or electrodeposition [15]. In polymer-CNT composites, both critical exponents and fractal dimension parameters are governed by kinetic processes (e.g., irreversible particle adhesion [9]) and percolation thresholds [4, 5], which directly affect the mechanical and electrical properties. Therefore, calculating these parameters provides fundamental insight into how nanofillers alter clustering, growth, and intercluster connectivity during synthesis.

There is also a relationship between the number of cluster sizes formed by cumulative pixels in structure and the rms value. This relationship can be determined from the observed hetero morphological projection layer and inter cluster spaced structure. At this stage of the study, in order to understand the cluster distributions and complexity degrees of the samples, the relationship between fractal dimensions $d_f(d, d_b)$ and critical exponent values can be calculated with the scaling approach

**Table 1** Primary and secondary critical exponent values of Rms values, constant and parameter values of the cluster-size distribution function for pure and SWCNT-doped samples, respectively

| Samples | Coverage ratio $\%P_{(i,j)}$ | 1. Critical exponent α | 2. Critical exponent β | γ | Fractal dimension $d_f(d=1)$ | Fractal dimension* $d_f$ |
|---|---|---|---|---|---|---|
| Pure | 45.91 | 1.705± 0.158 | 0.481± 0.029 | 0.426± 0.031 | 1.546± 0.029 | 1.859± 0.014 |
| Regression coefficient | - | 0.94113 | 0.97234 | 0.97645 | - | 0.99979 |
| Uncertainty (%) | - | 9.2 | 0.056 | 5.3 | | 1.0 |
| SWCNT | 47.99 | 1.965± 0.117 | 0.519± 0.048 | 0.362 0.026- | 1.373± 0.020 | 1.900± 0.012 |
| Regression coefficient | - | 0.97234 | 0.94113 | 0.97776- | - | 0.99987 |
| Uncertainty (%) | - | 5.9 | 9.2 | 7.1 | - | 1.0 |

*Box-counting method

suggested by Meakin [9]. If the relationship between the rms $T_s(h)$ thickness value and the formation number N (h) value is defined as follows:

$$N(h) \sim T(h)^{-\gamma} \tag{15}$$

where γ is the critical exponent for $d_f(d, d_b)$. Figure 6 shows the change in the number of clusters of the pure composite and the CNT-doped sample depending on the rms roughness value.

The relationship between the critical exponent value and the fractal dimension is defined as follows:

$$d_f(d, d_b) = d_f(d) - d_b \tag{16}$$

where $d_f$ (d) is the fractal dimension in d-dimensional space. The expression $d_f(d, d_b) = d_f$ also shows the fractal dimension of the carbon nanotube structuring under the boundary conditions in fiber and epoxy. In order to obtain optimum reliability in linear regression calculations, large values that disrupt the statistical distribution were ignored. For results showing scaling behavior in determining the data distribution, critical exponents were estimated at values of $r^2 > 0.97$, which is the largest value of the regression coefficient. The critical exponent values corresponding to the surface structure of pure and CNT-doped nanocomposites are 0.546 and 0.373, respectively. The critical value decreases when CNT is added as can be seen from the results. This is an expected result and shows that CNT particles disperse among the cluster structures forming the sample, reducing the distance. In addition, using the box counting algorithm, the fractal dimension was calculated as 1.859 for the neat sample and 1.90 for the CNT-doped sample. The results of the samples are summarized and presented in Table 1.

When the literature was examined, the critical exponent value for the growth of one-dimensional particles on two-dimensional surfaces, based on the DLA model, was reported as 1.30 by Meakin [9]. The critical exponent value of the zinc tree structure formed by the electrodeposition method on the linear electrode varies in a wide range between 1.43 and 1.67 [16]. The critical exponent value for nickel phosphate

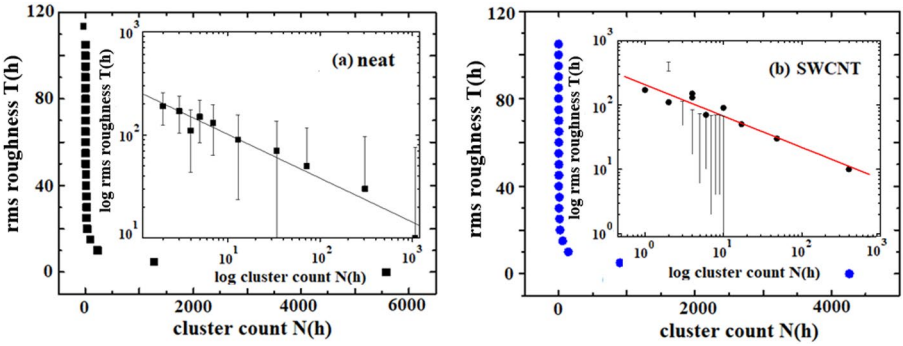


**Fig. 6** The variation of the cluster counts with rms roughness (**a**) Neat composite (**b**) CNT-doped sample

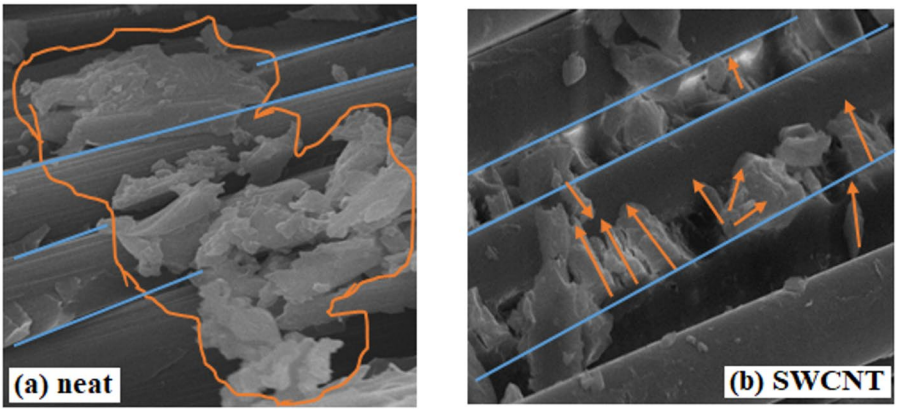


**Fig. 7** (**a**) Cluster structures on the surface of the pure sample, (**b**) Cluster structures on the surfaces of the doped composite. During the production process, the aggregated additives form perpendicular to the surface like an electrode

(Ni-P) electrodeposition structuring was calculated to be around 0.90 by Saitou et al. [15]. The critical exponent value obtained is quite small compared to both the DLA structuring simulation results and the Ni-P surface structuring.

The production temperature of the additive composite is lower than the melting temperature of the fiber. Therefore, the mobility of added polyester, resin and carbon nanotubes increases at the production temperature. Thus, the cylindrical fiber pieces in the sample act as linear electrodes and a thicker and irregular structure occurs compared to the zinc metal growth in a direction approximately perpendicular to the slurry fiber surfaces. Figure 7(a) shows the structuring on the fiber for the pure sample, and 7(b) shows the CNT-doped composite fiber surface and a micro image of the structuring between them. Fiber projection surface boundaries, which are observed as cylindrical structures in the structure, are shown with blue linear lines and cluster structures approximately perpendicular to them are shown with orange arrows. The structuring for both samples is irregular. Racz et al. proposed that 2D diffusion-limited deposition on a one-dimensional electrode can be determined by two exponents of scaling behavior referencing computer simulations, and the general deposition problem [14]. The variation of the independent cluster size on the cluster surface according to the number of clusters is given by the following relation:

$$N\ (s_i)\ \sim\ s^{-\tau}\, f\left(N^{-1}s^{\sigma}\right) \tag{17}$$

where N is the total number of independent clusters in the system, and the inequality $\tau < 2$ is valid for a non-equilibrium system. This equation is the usual scaling Ansatz developed by determining analogously for systems far from equilibrium. For systems in equilibrium, values evolve unevenly. $f(\epsilon)$ is the boundary function and takes values $f(\epsilon) \approx 1$ for $\epsilon \ll 1$ and $f(\epsilon) \ll 1$ for $\epsilon \gg 1$. For DLA model clusters, Vicsek et al. proposed a dynamic scaling function for dynamic scaling definition [17]. However, the cluster structure in the systems defined in Ref [17]. and Ref [18]. has an integrated symmetric or partially symmetric structure with diffusion effect. The composite structure

examined in this study is quite different from the structures available in the literature in terms of structure and production process. Coalescence with thermal effect and aggregation mainly with sedimentation behavior took place. It is observed that agglomeration in pure material mainly occurs when non-fiber production materials come together in irregular piles. In the structure formed by CNT doping, regional changes are observed. This indicates that deterministic components are effective in some regions and stochastic components in others. Accordingly, while factors such as pressure, temperature, and fiber orientation determine the macromorphology during sample growth (Fig. 3), the diffusion, distribution, and aggregation of CNTs within the resin contribute to the nanoscale morphology. This distribution of CNTs exhibits Poisson statistics due to thermal fluctuations (Eq. 13). This binary model can explain random aggregation in systems with deterministic boundaries.

Considering the limitations of the statistical analysis method used, it introduces an error of ± 3% in fractal dimension calculations, especially in SEM images with sub-8-bit resolution [13]. Furthermore, >±10% changes in the production parameters of the materials also significantly alter cluster statistics [4]. In this study, control measurements at different magnifications (2,000x-8,000x) determined that the critical α exponent varied by < ± 4%. This value proves that the method yields significant results under certain conditions.

In this study, the clustering states on the surface morphologies of both pure and nanotube-doped materials are investigated in detail numerically using fractal structuring, statistical scaling, and cluster distribution functions. Although direct mechanical, electrical, or thermal tests were not performed on the materials, previous studies indicate that such fractal structures effectively affect the macroscopic performance of the composites. Kozlov et al. [4], using the percolation threshold approach used to describe carbon nanotube network structures, showed that the material morphology affects and increases the hardness of the polymer matrix. Similarly, in another study by Bayırlı [8], it was shown that fractal morphologies can increase mechanical strength by affecting the microstructure within the material. In this context, it is anticipated that the clustering density observed on the surface and the increased fractal dimension may have positive effects on mechanical properties such as tensile strength and Young's modulus, particularly through the load transfer mechanism. Analysis of such structures can enable more effective dispersion and orientation of nanotubes within the resin matrix. Controlling the behavior of nanotubes can improve the electrical conductivity mechanism while strengthening the material integrity in mechanical terms.

## Conclusions

In this study, the irreversible structuring and surface morphology of pure and single-walled carbon nanotube-doped nanocomposites produced by the SMC technique were determined by numerical approaches using the scaling method. For this purpose, primary and secondary critical exponent values are calculated for rms roughness and regions showing scaling behavior according to rms roughness, taking as reference the cluster projection area observable on the SEM images of the samples.

In both examples, the surface structure shows polymorphological and heterogeneous features. Critical exponents and fractal dimensions were calculated for the samples by taking rms roughness and size frequency as reference. Values determined by the box-counting algorithm were used for comparison. It has been demonstrated that the cluster distribution on the surface exhibits exponential behavior. It has been determined that this irreversible cluster structuring occurs in a Poisson distribution process. Moreover, taking this finding as reference, the numerical cluster-size distribution function for the samples was defined and proposed as a numerical model.

**Author contributions** The authors declare that they have no conflict of interest.

**Funding** This research article received no grant from any funding agency in the public, commercial, or not-for-profit sectors.

**Data availability** This research contains no associated data.

## Declarations

**Ethics approval and consent to participate** The study does not include human or animal subjects.

**Consent for publication** The authors give their consent for publication.

**Conflict of interest** The authors declare that they have no conflict of interest.

## References

1. Țălu Ș (2015) Micro and nanoscale characterization of three dimensional surfaces. Basics and applications. Napoca Star Publishing, pp 21–28
2. Rempe AS, Stuefer M, Kindersberger J, Wagenbauer K, Ketterer P, Dietz H (2019) Quantification of the three-dimensional nanoparticle distribution in polymer nanocomposites. IEEE Trans Dielectr Electr Insul 26(2):601–609
3. Browning LA, Watterson WJ, Happe E, Silva SR, Valenzuela RA, Smith JH, Dierkes MP, Taylor RP, Plank NO, Marlow CA (2021) Investigation of fractal carbon nanotube networks for biophilic neural sensing applications. Nanomaterials 11(3):636
4. Kozlov GV, Dolbin IV (2018) Effect of a nanofiller structure on the degree of reinforcement of polymer–carbon nanotube nanocomposites with the use of a percolation model. J Appl Mech Tech Phys 59:765–769
5. Serban BC, Cobianu C, Dumbravescu N, Buiu O, Bumbac M, Nicolescu CM, Cobianu C, Brezeanu M, Pachiu C, Serbanescu M (2021) Electrical percolation threshold and size effects in polyvinylpyrrolidone-oxidized single-wall carbon nanohorn nanocomposite: the impact for relative humidity resistive sensors design. Sensors 21(4):1435
6. Sun C, Li F, Ying Z, Liu C, Cheng H (2004) Surface fractal dimension of single-walled carbon nanotubes. Phys Rev B 69:033404/1–4
7. Lee RI, Rizaeva YN, Manaenkov KA, Psarev DN, Kiba MR (2020) The fractal approach and the effect of nanoadhesive in polymer nanocomposites, IOP Conf. Ser : Mater Sci Eng 919:022042
8. Bayirli M (2014) Numerical approaches of cluster statistics for stochastic manganese deposits. Zeit für Naturfor A 69:581–588
9. Meakin P (1984) Diffusion-controlled deposition on surfaces: cluster-size distribution, interface exponents, and other properties. Phys Rev B 30:4207
10. Ilgaz A, Bayırlı M (2024) Fractal characterization for conductivity mechanism of single-walled carbon nanotube doped composites. Ind J Phys 98:1335–1341

11. Witten TA, Sander LM (1983) Diffusion-limited aggregation. Phys Rev B 27:5686–5697
12. Kartha MJ (2025) Diffusion limited aggregation of polymers with anisotropic interactions and phase transition. Appl Phys A 131:507
13. Schneider CA, Rasband WS, Eliceiri KW (2012) NIH image to imageJ: 25 years of image analysis. Nat Methods 9:671–675
14. Karperien A, FracLac for ImageJ (2012) Vers. 2.5w. Available at: http://rsb.info.nih.gov/ij/plugins/fraclac/fraclac-manual.pdf
15. Saitou M, Okudaira Y (2004) Macro internal structure of porous Ni-P electrodeposited under galvanostatic conditions. J of Electrochem. Soc. 151(10):674–679
16. Matsushita M, Hayakawa Y, Sawada Y (1985) Fractal structure and cluster statistics of zinc-metal trees de- posited on a line electrode. Phys Rev A 32:63814
17. Vicsek T, Family F (1984) Dynamic scaling for aggregation of clusters. Phys Rev Lett 52(19):1669–1672
18. Rácz Z, Vicsek T (1983) Diffusion-controlled deposition: cluster statistics and scaling. Phys Rev Lett 51:2382